

Resonance states of two-electron quantum dots

M. Bylicki, W. Jaskólski, and A. Stachów
Instytut Fizyki UMK, Grudziądzka 5, 87-100 Toruń, Poland

J. Diaz

Departament de Ciències Experimentals, UJI, Box 224, E-12080 Castelló, Spain

(Received 23 March 2005; revised manuscript received 29 June 2005; published 23 August 2005)

Autoionizing resonance states of two-electron quantum dots are studied by using the effective-mass complex-eigenvalue equation approach. It is shown that two-electron quantum dots may have very rich spectra of resonance states. The number of them and their lifetimes depend strongly on the dot size. It is observed that a resonance state may change its character from Feshbach to shape type with the dot size decreasing. Since the resonance states may have very long lifetimes they should not be neglected in the description of transport processes in quantum dots.

DOI: 10.1103/PhysRevB.72.075434

PACS number(s): 73.22.-f, 31.25.Jf

I. INTRODUCTION

Quantum dots are often called artificial atoms, since they exhibit many electronic and optical similarities to atoms. In particular, a few-electron QD system may exist in quasi-bound states like the autoionizing states of atoms. Although the autoionizing states of a few electron atoms have been intensively studied for the last four decades,¹ very little has been done for the resonance states of quantum dots. Only one-electron resonances have been investigated.^{2,3}

So far, most of the investigations of many-electron quantum dots were focused on bound states. This is a consequence of the parabolic confining potential, that was most commonly used in the research. Such a potential describes quite well the lowest energy states of a quasi-two-dimensional quantum dot (especially in a magnetic field).⁴⁻⁷ Unfortunately, for large distances from the dot center the harmonic oscillator potential is unphysical and is useless in the modelling of resonance autoionizing and tunnelling states of quantum dots. The number of papers involving asymptotically finite potentials is rather limited.⁷⁻⁹ All these works were devoted to the bound states exclusively.

However, applications of quantum dots, e.g., electron or spin transmission nanodevices,¹⁰ require precise description of scattering (tunnelling) many-particle states of excess electrons in semiconductor quantum dots. In this paper we initiate the investigation of the resonance autoionizing states of two-electron quantum dots.

II. THE QUANTUM DOT MODEL

The model of quantum dot we consider is of spherical symmetry. The electrons are confined in a finite rectangular potential well

$$V(r) = \begin{cases} -V_0, & r < R, \\ 0, & r \geq R \end{cases} \quad (1)$$

of the depth V_0 and of the radius R . Such a model describes well a quantum dot built of a narrow-gap semiconductor nanocrystal of radius R , surrounded by a wide-gap semicon-

ductor (or a dielectric medium) with the conduction band off-set equal to V_0 .

We work within the one-band effective-mass approximation. For simplicity we assume that the effective mass, m^* , and the dielectric constant, ϵ , are uniform within the whole structure. The Hamiltonian for two electrons confined by the potential V (two excess electrons in the conduction band energy range of the quantum dot) is

$$H = -\frac{\hbar^2}{2m^*}\Delta_{\mathbf{r}_1} - \frac{\hbar^2}{2m^*}\Delta_{\mathbf{r}_2} + V(r_1) + V(r_2) + \frac{e^2}{\epsilon|\mathbf{r}_2 - \mathbf{r}_1|}. \quad (2)$$

We use units of the effective Rydberg, $R_0 = m^* \kappa^2 e^4 / 2\hbar^2 \epsilon^2$ and the effective Bohr radius $a_0 = \epsilon \hbar^2 / m^* \kappa e^2$, where $\kappa = 1/4\pi\epsilon_0$, ϵ_0 is the vacuum permittivity and e is the electron charge. The depth of the potential well has been taken as $V_0 = 10R_0$. For typical values of $m^* = 0.1m_e$ and $\epsilon = 5$, which we use in our computation, V_0 results to be ~ 0.54 eV. This fits well (the order of magnitude) the conduction band off-sets typical for semiconductor quantum dots. We have performed a series of calculations for the quantum dot size from ~ 1.5 nm to ~ 40 nm, covering the size-range of chemically synthesized nanocrystals.^{11,12}

This choice of the parameter values is due to the practical (experimental) reasons as given above. The other reason is that computations for the bound states of such systems were recently performed by Szafran, Adamowski, and Bednarek⁸ and by Varga, Navratil, Usukura, and Suzuki.⁷ So we can discuss our bound-state results in the context of those works. Also our investigations of resonances can be considered as a continuation of those works.

III. METHOD OF COMPUTATION

We are interested in both the bound and resonance eigen-solutions of

$$H\Psi = E\Psi, \quad (3)$$

for the Hamiltonian given in Eq. (2). We obtain approximations to them by performing variational calculations involving a CI-type trial expansion,

$$\Psi = \sum_k c_k \psi_k, \quad (4)$$

where the two-electron configuration functions,

$$\psi_k = \Lambda \phi_{k_1}(\vec{r}_1) \phi_{k_2}(\vec{r}_2) \chi_{S, M_S} \quad (5)$$

are constructed of Slater-type orbitals (STOs), $\phi_{k_i}(\vec{r})$. The two-electron spin function is represented by χ_{S, M_S} . Λ stands for all the operations necessary to couple the angular momenta and to antisymmetrize the total function.

The usual CI approach is suitable for the bound states. For resonances we use the complex-eigenvalue Schrödinger equation (CESE) approach¹³ as it is described in Ref. 14. The method is based on two fundamental properties of resonance eigenfunctions of Eq. (3): First, since resonance state is an initially bound state of the system which decays by ejecting one electron, the resonance eigenfunction has a specific asymptotic behavior. The escaping electron being far away from the remaining part of the system is described by an outgoing wave only. The incident wave is absent. Second, such a specific boundary condition implies that the corresponding eigenvalue is complex with the imaginary part negative, $E = E_r - i\Gamma/2$. The real part of a resonance eigenvalue is the position of the center of quasiscrete resonance energy level. The imaginary part corresponds to the half-width, Γ , of such a broadened level. Since Γ is a measure of the probability of the decay per unit of time, it determines the lifetime of the metastable resonance state as $\tau = \hbar/\Gamma$.

Another constituent of the CESE approach is the complex coordinate rotation transformation, $\vec{r} \rightarrow \vec{r}e^{i\theta}$, where θ is a real parameter. The outgoing wave transforms under the complex coordinate rotation into a square-integrable function. This implies that after the complex rotation the resonance eigenfunction can be found in the space of square integrable functions, as the bound state functions are. Which is suitable from a computational point of view.

The practical CESE prescription is the following: The trial expansion (4) is divided into two parts. One is to describe the localized character of a resonance. The configuration functions, ψ_k , belonging to this part are of the usual form, Eq. (5), proper for bound states. The role of the other part is to take the asymptotics of resonance states into account. In those configurations, STOs representing the outgoing (free) electron are complex rotated,

$$\psi_k = \Lambda \phi_{k_1}(\vec{r}_1) \phi_{k_2}(\vec{r}_2 e^{-i\theta}) \chi_{S, M_S}. \quad (6)$$

This basis set leads to a non-Hermitian Hamiltonian matrix problem dependent on the complex-rotation angle θ which is considered as a variational parameter. Thus the matrix eigenproblem is solved repeatedly for various values of θ . The complex eigenvalues that stabilize against θ variation correspond to resonances. Their real and imaginary parts are interpreted as given above.

In our computations the length of the expansion (4) was 1531 for the $^1S^e$ states, 1630 for the $^3S^e$ states and 2560 for both singlet and triplet P^0 symmetries. The configuration functions were made of 20 unrotated STOs of each s , p , d , f , and g angular type. The number of complex rotated STOs

was 21 of each applicable angular type. The complex rotation parameter was varied from 0 up to 0.7 in steps of 0.05. The exponent parameters of STOs were partially optimized for $R = 1a_0$, $8a_0$, and $15a_0$. Since they seemed to fit exponential dependence on R the interpolated values were used for QDs of other sizes.

IV. RESULTS

A wide spherical well of the radius of a 10 or so a_0 supports many one-electron bound states of various angular momentum values. In the one-electron picture, they lead to a manifold of bound two-electron states, which is rich regarding the number of states as well as the variety of $^{2S+1}L^\pi$ symmetries (L is the total angular momentum quantum number, S is the total spin, and π indicates the parity). For smaller quantum dots the binding is weaker and the number of bound states is smaller. With the quantum dot radius decreasing, each two-electron bound level approaches the continuum threshold determined by the $1s$ or $1p$ one-electron levels, respectively, for the states of $\pi = (-1)^L$ or $\pi = (-1)^{L+1}$ parity ($\pi = 1$ is for even states and $\pi = -1$ is for odd states; hereafter we use e and o to label *even* and *odd* states, respectively). Eventually, for some critical R , specific to a given two-electron state, its level crosses over the threshold and enters into the continuum. The state is no longer bound because the electron correlation mixes the bound configuration of the state under consideration and the unbound electron configurations which now correspond to the same energy.

This quite obvious qualitative picture has been confirmed by quantitative computations of Szafran, Adamowski, and Bednarek.⁸ They followed the changes of bound levels with respect to decreasing R until they had reached the $1s$ continuum threshold. The aim of the present paper is to follow the levels further, when they are embedded in the continuum. We consider the $^1S^e$, $^3S^e$, $^1P^o$, and $^3P^o$ states.

A. Bound state energies

We also have performed computations for the bound states. The reason for computing them was to check the accuracy of our computation. This could be done by comparing our results to the data of Szafran *et al.*⁸ and Varga *et al.*⁷ In both works the electron correlation effects were taken into account by using efficient variational methods implementing correlated trial functions. Unfortunately, the presumably accurate results of Varga *et al.* are presented in a figure (Fig. 7 of Ref. 7) of poor resolution so that no quantitative comparison is possible. As regards the work of Szafran *et al.* one can read their results for $R = 15a_0$ from their Fig. 4. Those results are compared to ours in Fig. 1. It is seen that our energy levels of the bound states are significantly lower, than those of Ref. 8. This means that the variational CI wave functions, as used in this paper, represent better the electron correlation effects than the r_{12} -correlated functions, as used in Ref. 8 (although in principle the latter are more powerful).

Several differences in the sequence of levels are also well seen in Fig. 1. One of them should be emphasized, for QD as

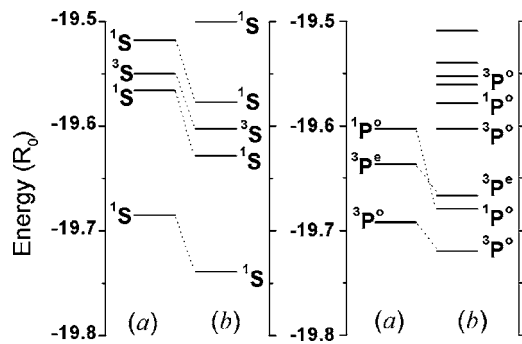


FIG. 1. Several lowest energy levels of the two-electron QD of radius $15a_0$. (a) Reference 8, (b) this work.

large as $R=15a_0$ the ground two-electron state is of the $1S$ symmetry as it is for smaller QDs, and not of $3P^o$ symmetry as obtained in Ref. 8.

The issue of the symmetry of the ground state of a two-electron QD was discussed in the literature.^{6,7,15} In 1996, Fujito¹⁵ suggested that for a parabolic confinement the symmetry of the ground state changes from singlet to triplet when the size of the dot increases. Then, this opinion was denied by Szafran *et al.*,⁶ who proved that for a parabolic confinement, the ground state has always singlet-spin symmetry and that the results of Ref. 15 suffered from the neglect of the correlation effects. However, based on their numerical results and theoretical discussion confined to harmonic potentials, Szafran *et al.*⁶ could not judge definitely whether the “singlet-triplet phase transition” observed in Ref. 8 was a fictitious effect due to incomplete inclusion of the electron correlation. So they left this question open. The problem was undertaken by Varga *et al.*⁷ Among many other systems they considered two electrons in the confining potential of a finite depth, as the one of Eq. (1), used in the present work and in Ref. 8. Varga *et al.* observed no level crossing between the lowest triplet and singlet states. The result of Szafran *et al.*⁸ was not confirmed. However, because of the resolution of Fig. 7 of Ref. 7 where the results of Varga *et al.* are presented, it is impossible to state whose results, these of Ref. 7 or those of Ref. 8, are more accurate and reliable, and which is the physically right result. The comparison in Fig. 1 of our results with those of Ref. 8 makes legitimate the conclusion that the ground state of two electrons confined in the potential (1) is a singlet S state, independently of the dot size (up to $R=15a_0$).

B. Resonance states

Let us turn now to our main interest, to resonance states. In Figs. 2(a) and 2(b), respectively, the energies of the S^e and P^o levels are plotted versus the QD size, R , in the range from $0.5a_0$ up to $2.5a_0$. They are labeled with the leading electron configurations. A few low lying one-electron levels are also plotted. They serve as thresholds for continua of unbound two-electron state energies. In particular, the $1s$ one-electron level constitutes the critical energy position above which the localized two-electron states presented in this work (i.e., of the S^e and P^o symmetries) are not strictly bound but reso-

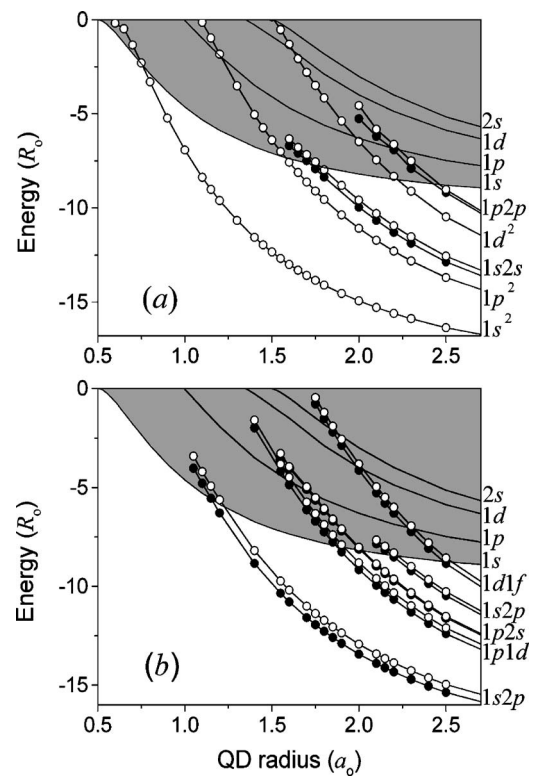


FIG. 2. Energies of two-electron bound and resonance states vs dot radius, R . (a) and (b) are for S^e and P^o states, respectively. Open circles are used for singlet states and full points for triplet ones. The levels are labeled with the leading electron configurations. The $1s$, $1p$, and $1d$ one-electron levels constitute continua thresholds. The area above the $1s$ level is shadowed to indicate the energy continuum.

nant. In order to emphasize this, the area above the $1s$ line is shadowed. One can see that after crossing over the $1s$ threshold the two-electron resonance level lines continue within some range of decreasing R . Then they disappear for small R . Apparently the disappearance of a given two-electron resonance is correlated with the fact of the disappearance of one of those one-electron bound states which are involved in the electron configuration under consideration. For instance, the $1s2s1S^e$ and $3S^e$ resonances do not show up for $R < 1.55a_0$, in Fig. 2(a), because the $2s$ one-electron state does not exist for such small QDs. The $1s2s$ levels disappear in the $1s\epsilon s$ continuum (corresponding to the one-electron bound in the $1s$ state and the other electron free and having the kinetic energy ϵ and the orbital angular momentum $l=0$). They do not get into another one. Some other two-electron energy levels cross the higher one-electron levels, nl , and enter into next continua, $nl\epsilon l'$. For example, the $1d1f3P^o$ level crosses the $1p$ threshold at $R \approx 2.28a_0$, then it crosses the $1d$ and $2s$ thresholds at $R \approx 1.98a_0$ and $R \approx 1.84a_0$, respectively.

Having the energy levels embedded in multiple continuum, the resonance states may decay in many channels, each one connected to one continuum $nl\epsilon l'$. Decay in the $nl\epsilon l'$ channel consists in ejection of one electron with the kinetic energy ϵ and the angular momentum l' and leaving the other electron in the nl bound state. Following the con-

cept of artificial atom, such a decay process may be called autoionization.

The probabilities of autoionization per unit of time, given by the widths Γ , are presented in Fig. 3. The autoddecay probability of a state having the critical energy position at the $1s$ threshold, is equal to zero. The width increases monotonically when the resonance level is getting deeper into the continuum (higher above the $1s$ threshold; when R is decreasing). The dependence of the width on the QD size is specific to a given state. In particular, it depends on the relation between the leading electron configuration of the resonance and the configurations belonging to the continuum. Let us discuss the $^1S^e$ resonances shown in Fig. 3 (the most upper part). The widths of the $1s^2$ and $1s2s$ states behave in a way similar to each other, they increase rapidly but smoothly with decreasing R . These two localized states are strongly coupled to the $1s\epsilon s$ unbound continuum states. Therefore their widths reach quickly large values of about 10^{-2} eV. Both levels disappear before reaching next continuum threshold.

The behavior of the widths of the $1p^2$ and $1d^2$ $^1S^e$ states is different (see Fig. 3). These states are weakly coupled to the $1s\epsilon s$ continuum. After a rapid increase, corresponding to the position just above the $1s$ threshold, the widths stabilize at values of the order of 10^{-4} eV. Only after getting into the $1p\epsilon p$ continuum the width of the $1p^2$ level jumps up and the level disappears soon (for the QD size for which the one-electron $1p$ state gets lost). The opening of the $1p\epsilon p$ continuum does not affect significantly the width of the $1d^2$ level. It increases a bit and then remains stable at 3×10^{-4} eV until the level has reached the $1d\epsilon d$ continuum at $R=1.62a_0$. These continuum states are closely related to the $1d^2$ configuration. There is strong coupling between them. Hence, the width increases rapidly for $R < 1.6a_0$.

The relationship between the continuum electron configurations and the resonance configuration is the main criterion for distinguishing between the so-called Feshbach and shape resonances. The ones whose configurations are closely related to the configurations of the continuum in which they are embedded, are of the shape type. They decay easily and their widths are large. The configuration of a Feshbach resonance is not related to the background continuum configurations.^{16,17} Hence the decay must involve reconfiguration of the system remaining after autoionization. Therefore, the lifetimes of Feshbach resonances are relatively longer than those of shape resonances. As one can see from the discussion above, in our system we have resonances of both categories. Moreover, most of them change the character from Feshbach to shape when the QD size decreases and the levels enter into the proper continua. One can state that every resonance evolving down the QD size starts as a bound state and reaches the shape stage before disappearing. Those of $1snl$ configurations miss the Feshbach phase.

The Feshbach and shape resonance concepts are simplified models only. Real complex systems are more complicated due to the electron-correlation effects mixing the open and closed channels. Nevertheless, from the discussion above it is seen how well these models work in the present case. It is also interesting to observe how the character of a given state changes versus the size parameter. Such changes

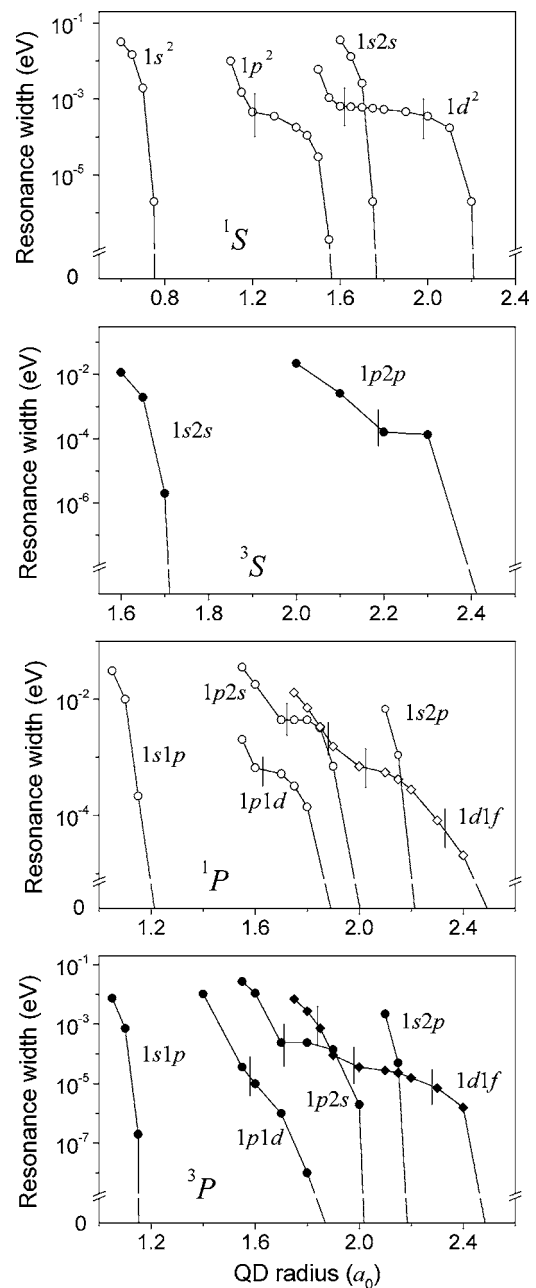


FIG. 3. Widths of two-electron resonance levels vs the QD radius R . The consecutive figures are for the $^1S^e$, $^3S^e$, $^1P^o$, and $^3P^o$ resonances. The labels and open and full symbols are used as in Fig. 2. Diamonds are used for the $1d1f$ states so as to avoid confusion. The resonance width is equal to zero for the critical value of the QD size, proper for a given state. (The curves start at those points.) Vertical bars placed on a given line indicate the QD size values for which the corresponding resonance level crosses the excited one-electron levels (these are consecutively the $1p$, $1d$, and $2s$ levels) and enters higher continua. Drastic change of the slope of the line associated with such a crossing over the threshold is due to the Feshbach-to-shape change of the resonance character. This does not happen to the $1snl$ states, they omit the Feshbach phase.

also occur in other systems, e.g., along an isoelectronic atomic sequence, where the atomic number is the key parameter. An electron configuration which leads to a Feshbach

resonance in the case of neutral atom (of atomic number Z) can lead to a shape resonance in the isoelectronic negative ion ($Z-1$). In computations one can change the atomic number in a “continuous” way from Z down to $Z-1$ and observe how the character of the state changes. However, this cannot be done experimentally. Unlike the true atoms, the artificial ones—quantum dots—can be fabricated with the size control down to a single monolayer (≈ 0.3 nm), e.g., chemically synthesized nanocrystals.¹² Thus, it is possible to produce such QDs that their size values cover quite densely the range of R investigated in present work. This makes an experimental investigation of changes discussed above possible, provided the experiment is capable of seeing the resonance levels. We believe that the experiments like those performed by Klein *et al.*¹⁸ and Banin *et al.*,¹⁹ where single electrons were transmitted through QDs, could be used for this purpose.

V. CONCLUSION

We have performed computations for two-electron quantum dot bound and resonance states. We have obtained results with the accuracy which allows us to state that the ground two-electron state is of the singlet S^e symmetry, in the wide range of size of the investigated quantum dots (up to $15a_0$).

Decreasing the QD size we followed the transformation of two-electron bound states into Feshbach and then into shape resonances. The widths of resonance levels increase monotonically with the decreasing QD size. Eventually, each resonance disappears if QD is small enough. The size of QD critical for such a disappearance is specific to a given state. It is correlated with the size at which the one-electron states needed for the one-configuration description of the resonance under consideration turn to be unbound.

The largest widths we obtained were about 10^{-2} eV, corresponding to the lifetimes of the order of 10^{-13} s. On the other hand, the lower limit for the widths is zero, which means that a given resonance can live arbitrarily long provided QD is of proper size. Thus the existence of resonances should not be neglected if the electron transport processes in QDs are considered.

In our opinion our theoretical findings can be confirmed by single-electron-transmission experiments. We also believe that our results may be helpful in tailoring the transport properties of QD-based nanodevices by selecting the QD size.

ACKNOWLEDGMENTS

Financial support from KBN-3T1104326 and PZB-MIN-008/P03/2003 is gratefully acknowledged.

-
- ¹S. J. Buckman and C. W. Clark, *Rev. Mod. Phys.* **66**, 539 (1994); M. Bylicki and E. Bednarz, in *Explicitly Correlated Functions in Chemistry and Physics*, edited by J. Rychlewski (Kluwer Academic, Dordrecht, Boston, London, 2003); M. Bylicki, *Adv. Quantum Chem.* **32**, 207 (1998).
- ²R. Buczko and F. Bassani, *Phys. Rev. B* **54**, 2667 (1996).
- ³M. Bylicki and W. Jaskólski, *Phys. Rev. B* **60**, 15924 (1999).
- ⁴L. Jacak, P. Hawrylak, and A. Wójs, *Quantum Dots* (Springer, Berlin, 1998).
- ⁵R. M. G. Garcia-Castelan, W. S. Choe, and Y. C. Lee, *Phys. Rev. B* **57**, 9792 (1998).
- ⁶B. Szafran, J. Adamowski, and S. Bednarek, *Physica E (Amsterdam)* **5**, 185 (2000).
- ⁷K. Varga, P. Navratil, J. Usukura, and Y. Suzuki, *Phys. Rev. B* **63**, 205308 (2001).
- ⁸B. Szafran, J. Adamowski, and S. Bednarek, *Physica E (Amsterdam)* **4**, 1 (1999).
- ⁹S. Bednarek, B. Szafran, and J. Adamowski, *Phys. Rev. B* **59**, 13036 (1999); J. Adamowski, M. Sobkowicz, B. Szafran, and S. Bednarek, *ibid.* **62**, 4234 (2000).
- ¹⁰*Semiconductor Spintronics and Quantum Computation*, edited by D. D. Awschalom, D. Loos, and N. Samarth (Springer, Berlin, 2002); L. P. Kouwenhoven, D. G. Austing, and S. Tarucha, *Rep. Prog. Phys.* **64**, 701 (2001).
- ¹¹R. B. Little, M. A. El-Sayed, G. W. Bryant, and S. Burke, *J. Chem. Phys.* **114**, 1813 (2001).
- ¹²A. Mews, A. V. Kadavanich, U. Banin, and A. P. Alivisatos, *Phys. Rev. B* **53**, R13242 (1996).
- ¹³C. A. Nicolaides, *Int. J. Quantum Chem.* **60**, 119 (1996).
- ¹⁴M. Bylicki, W. Jaskólski, and R. Oszwałdowski, *J. Phys.: Condens. Matter* **8**, 6393 (1996).
- ¹⁵M. Fujito, A. Natori, and H. Yasunaga, *Phys. Rev. B* **53**, 9952 (1996).
- ¹⁶H. Feshbach, *Ann. Phys. (Leipzig)* **19**, 287 (1962).
- ¹⁷M. Bylicki, *Phys. Rev. A* **40**, 1748 (1989).
- ¹⁸D. L. Klein, R. Roth, A. K. L. Lim, A. P. Alivisatos, and P. L. McEuen, *Nature (London)* **389**, 699 (1997).
- ¹⁹U. Banin, Y. W. Cao, D. Katz, and O. Millo, *Nature (London)* **400**, 542 (1999).